Chiang Mai J. Sci. 2018; 45(5) : 2059-2068
http://epg.science.cmu.ac.th/ejournal/
Contributed Paper

Preparation and Properties of Polylactide Bio-composites with Surface-modified Silica Particles

Narisara Jaikaew [a], Atitsa Petchsuk [b] and Pakorn Opaprakasit* [a]

[a] School of Bio-Chemical Engineering and Technology, Sirindhorn International Institute of Technology (SIIT), Thammasat University, Pathum Thani, 12121, Thailand.

[b] National Metals and Materials Technology Center (MTEC), Thailand Science Park, Pathum Thani, 12120, Thailand.

* Author for correspondence; e-mail: pakorn@siit.tu.ac.th

Received: 1 November 2017
Accepted: 30 April 2018

ABSTRACT

Biodegradable plastics have become interesting alternative materials in packaging applications, because of their lower environmental impacts. Among these, polylactide (PLA) has played a key role, pertaining to many of its excellent properties. However, its commercialization as packaging materials for products sensitive to light, gas, or temperature changes, such as fresh vegetables and fruits, is challenging, due to its moderate gas transmission rates, and lower mechanical properties, compared to conventional plastic products. One effective method to solve this problem is the adding of inorganic fillers to the PLA resin to improve its properties. In this study, PLA bio-composite films have been developed by introducing low-cost silica particles as a reinforcing agent. To effectively achieve property enhancements, compatibility between the 2 components needs to be improved. Surface modification of the inorganic silica particles is conducted by coating with poly (lactic acid-*grafted*-chitosan) copolymer (PCT). Commercial silica particles (*c*-silica), with average particle size of 1-5 μm, were coated with PCT copolymer, employing a phase inversion emulsification (PIE) technique. After the coating process, the average size of the modified particles (*m*-silica) decreases to 17 nm, as the coated PCT layers on the particle surfaces prevent agglomeration of the silica particles by providing steric repulsion. The resulting *m*-silica and *c*-silica are then used in the preparation of PLA/silica bio-composite films by varying silica types and their contents from 0-5.0 wt%. Thermal and mechanical properties, light transmission, and gas permeability of the 2 bio-composite systems, are compared. PLA/*m*-silica exhibit greater tensile behaviors at all particle compositions. Variations in CO_2/O_2 permeability of bio-composite films can be optimized by changing the silica compositions. At 5.0 wt% of *m*-silica, the highest decrease in light transmission at 4, 8, and 16% for UV-A, UV-B, and visible regions, respectively, are observed. The resulting PLA/*m*-silica bio-composite films have high potential for use as smart packaging for fresh vegetables and fruits.

Keywords: packaging, polylactide, silica particles, bio-composite, permeability, light transmission

1. INTRODUCTION

Biodegradable polymers have attracted vast interest, due to environmental awareness concerning global warming, rapid decrease of petroleum resources, plastic waste and pollution problems. Among these, polylactide or polylactic acid (PLA), a thermoplastic aliphatic polyester, is one of the most attractive environmental-friendly materials, due to its degradability, ease of processability, relatively low cost of production, renewability, and good mechanical strength [1, 2]. PLA can be synthesized by either polycondensation of lactic acid, or ring-opening polymerization (ROP) of lactide dimer, in which the latter is the most effective process to obtain high molecular weight PLA. However, the polymer exhibits poor thermal stability and low melt strength. This limits its use in several ways [3-6].

Addition of fillers to polymers, generating composite materials, is an effective method to improve their properties, especially for PLA [7, 8]. The property improvement is achieved by strong interactions between the filler's particles and the polymer matrix. Various composites of PLA with other biodegradable/biocompatible materials have been prepared to enhance its thermal and mechanical properties, but still retain its biocompatibility and degradability [9-11]. Many inorganic fillers have been used for preparing polymeric composite materials [12, 13]. Among these, silica (SiO_2) is one of the most popular, due to its low cost and highly abundance in nature [14]. There are many sources of silica such as sand, clay, and ash. PLA bio-composites have been widely studied by many researchers due to their unique properties, such as biodegradability, biocompatibility, good barrier property, low cost, and high modulus. However, modification of silica particles is required to improve the compatibility between the particles and the polymer matrix for achieving enhanced characteristics.

In our previous work, we have successfully prepared silica particles from rice husk ash (RHA) and modified their surfaces with poly(lactic acid-*grafted*-chitosan) copolymer (PCT) by employing a one-step coating method. The modified particles were used as fillers in the preparation of PLA/silica bio-composite films to enhance their mechanical properties and gas permeability for use as packaging materials [15].

In this study, surface modification of commercial silica particles is conducted by coating with PCT copolymer employing, a phase inversion emulsification (PIE). The technique provides micro- or nano-particles with a narrow particle size distribution, and low process cost [16]. The resulting modified silica particles (*m*-silica) are then used as reinforcing material for commercial PLA films. Thermal, mechanical, and light transmission properties, and gas permeability of the bio-composite films containing untreated commercial silica (*c*-silica) and *m*-silica, are compared. The materials are highly suitable for use in active packaging applications.

2. MATERIALS AND METHODS

2.1 Materials

Poly(lactic acid-*grafted*-chitosan) copolymer (PCT) was synthesized in this laboratory, according to the procedure previously reported [15]. Commercial silica (Sigma Aldrich, USA) with an average particle size of 1-5 μm, was used. In the phase inversion emulsification (PIE) process, poly(vinyl alcohol) (PVA) (Sigma Aldrich, USA; degree of hydrolyzed, 87-90%; molecular weight 3×10^4 g/mol) and sodium dodecyl sulfate (SDS; Sigma Aldrich, analytical reagent), were used as surfactants. Chloroform ($CHCl_3$), (Sigma Aldrich, analytical grade) was used as a solvent. Polylactide (PLA) 4043D pellets were purchased from Nature Works (USA) and used in the preparation of composite materials.

2.2 Experimental Methods

2.2.1 Preparation of modified silica particles (*m*-silica)

Modified silica particles (*m*-silica), coded as *m*-silica, were prepared by coating *c*-silica with PCT copolymer, employing a Phase Inversion Emulsification (PIE) method, in which aqueous and oil phases are prepared. The aqueous phase consists of 10 g *c*-silica particles, dispersed in 0.1 M NaOH solution containing SDS (12.5%wt of water). The oil phase contains 2.5 g of PCT copolymer and 2 g of PVA dissolved in $CHCl_3$ solvent. Both SDS and PVA act as surfactants, and migrate from the bulk to the interface, leading to a decrease in the interfacial tension. The water phase was added dropwise into the oil phase at a 1 ml/min rate, with continuous stirring at 500 rpm. When the water phase was completely added, a milky mixture was obtained, and the mixture was further stirred for 1 h. The mixture was then placed in a fume hood for one night to completely evaporate the $CHCl_3$ solvent. The sample was then centrifuged, where the precipitants were separated and dried in a vacuum oven at 60 °C for 24 h.

2.2.2 Fabrication of PLA/silica bio-composite films

The modified silica particles (*m*-silica) and commercial silica (*c*-silica) were blended with PLA by an internal mixer (Chareon Tut, Thailand) at 170 °C for 15 min. The contents of the particles were varied from 0.5 to 5.0 wt%. Films of neat PLA, PLA/*c*-silica, and PLA/*m*-silica were prepared by a compression molding machine (Chareon Tut, Thailand) at 170 °C for 15 min. The specimens were prepared in a rectangular sheet form, with a 15 mm width and 100 mm of gauge length for the tensile test according to ASTM D882. For the gas permeability test, films with an average thickness of 40-50 μm were prepared by the same method.

2.2.3 Surface studies of silica particles

Surface morphology of *c*-silica and *m*-silica particles was examined by SEM (JEOL-JSM-7800F). The samples were prepared by a goal coating technique. Surface chemical compositions of the materials were characterized by SEM, with energy dispersive X-ray analysis (EDX).

2.2.4 Characterization of bio-composite films

Thermal behavior of bio-composite films was studied by Differential Scanning Calorimetry (DSC822e Mettler Toledo). The evaluation was by a heat-cool-heat standard method from -20 to 200 °C, at a heating and cooling rate of 20 °C/min. The first heating step is employed to erase the sample's thermal history.

The degree of crystallization is calculated by the following equation:

$$Xc = \frac{\Delta H_m}{\Delta H_m^\circ} \times 100\%$$

Where, ΔH_m is the enthalpy of melting and ΔH_m° denotes the enthalpy of fusion for fully crystalline PLA, which has a value of 93.1 J/g [17].

Tensile behaviors of the bio-composite films at various particle compositions were studied by a Universal Testing Machine (T-series Materials testing machine, model H5TK, Tinius Olsen LTD., UK) equipped with a 100 N load cell, with a crosshead speed of 50 mm/min at ambient temperature. At least six specimens were examined for each test, and an averaged value was reported. Break energy of the samples was calculated from the area under the stress-strain curves.

Permeability tests of the bio-composite films were conducted. Oxygen permeability was recorded on a Mocon Instrument (Ox-Tran Model 2/21), following ASTM D3985, at 23 °C, 0% relative humidity. Carbon dioxide permeability was measured on a Mocon Instrument (Permatran-C Model 4/41), at 23 °C and 0% relative humidity. Water vapor permeability was measured on an Illinois Instrument (Model 7200), using ASTM F1249-01, at 38 °C and 90% relative humidity and 1 atm pressure. UV-Visible-Near IR transmittances of the composite films were determined by a spectrophotometer (Agilent Technologies, CARY 7000). The measurements were conducted from 250-2500 nm in the transmission mode.

3. RESULTS AND DISCUSSION

3.1 Surface Morphology of Silica Particles

Properties of silica particles before and after surface modification, in terms of size, shape, and surface morphology, are examined. In general, inorganic particles with hydrophilic hydroxyl groups can easily adhere to each other through a hydrogen bonding network, leading to the formation of aggregate. SEM images of *c*-silica and *m*-silica particles, at magnifications of 25000 and 50000X, are compared in Figure 1. Both *c*-silica and *m*-silica particles show an irregular shape. However, *c*-silica has a higher content of aggregate, compared to *m*-silica. This is likely because the PCT copolymer chains can act as polymeric surfactants by adsorbing on the surface of silica particles, interrupting physical interactions between silica particles. The average particle size of non-aggregated particles is determined from SEM images by using J-image software. The average sizes of *c*-silica and *m*-silica particles are 58 and 17 nm, respectively. The *m*-silica also shows more uniform size distribution than *c*-silica. These result from effective coating by the PIE method.

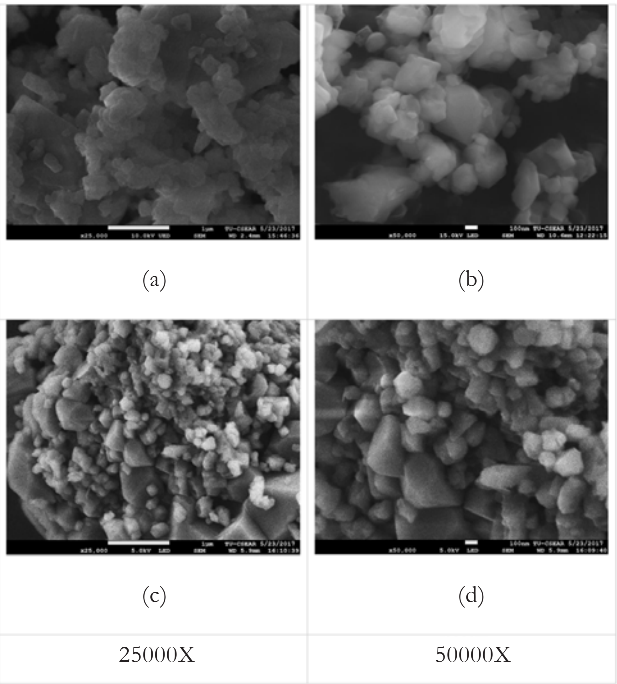

(a) (b)

(c) (d)

25000X 50000X

Figure 1. SEM images of (a), (b) *c*-silica and (c), (d) *m*-silica, at 25000 and 50000X magnification.

SEM-EDX results on surface compositions are summarized in Table 1, where 23.4 and 7.3 wt% Si contents are observed for *c*-silica and *m*-silica, respectively. The relatively lower weight percentages of Si and O atoms, and higher C content of *m*-silica reflect the presence of PCT copolymers on particle surfaces. It is expected that the remaining polymeric surfactant, present as a coating layer on particle surfaces, also plays a role in enhancing compatibility with the PLA matrix.

Table 1. Surface chemical compositions of *c*-silica and *m*-silica particles.

Elements	*c*-silica		*m*-silica	
	wt %	Atomic %	wt %	Atomic %
C	19.4	26.8	56.8	65.3
O	57.2	59.4	36.0	31.1
Si	23.4	13.8	7.3	3.6

3.2 Bio-composite Film Properties

Thermal properties of PLA, PLA/*c*-silica, and PLA/*m*-silica bio-composite films at various particles compositions were studied by DSC, as shown in Figures 2 and 3. All samples have a semi-crystalline structure, with glass transition temperature (T_g) at 60-62 °C, and crystalline melting temperature (T_m) at 149-151 °C. Cold crystallization (T_c) is observed at 119-124 °C. In addition, physical aging behavior is observed in all samples from their corresponding 1st heating scan thermograms, as a sharp peak located immediately following the glass transition. This is because the samples are stored in a desiccator at ambient temperature, with controlled humidity (%RH) of 25-50%, for 2 weeks before DSC testing. Physical aging is a natural phenomenon that significantly affects the physical properties of amorphous or glassy polymers (or polymers with T_g). During aging, the material becomes more and more glass-like and less rubber-like, i.e., stiffer and more brittle. The effects of aging takes place at temperatures below T_g, as the molecular mobility is not quite zero, with a slow and gradually approach to equilibrium. The change in physical properties with aging can have significant economic implications, and in some cases, it is necessary to predict long-term behavior from an accelerated short-time test. Permeability of packaging materials is also affected by physical aging.

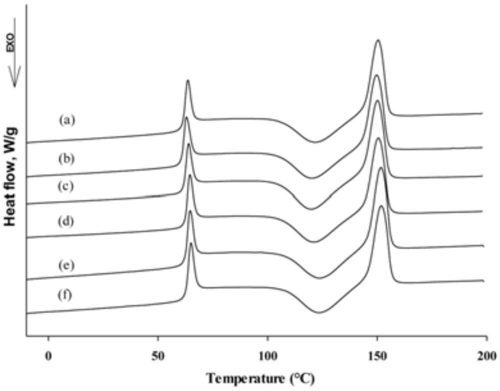

Figure 2. DSC thermograms (1st heating scan) of (a) PLA, and PLA/*m*-silica bio-composite films at various *m*-silica compositions: (b) 1.0, (c) 1.5, (d) 2.0, (e) 2.5, and (f) 5.0 wt%.

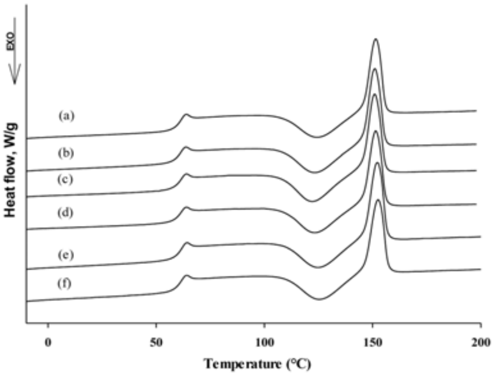

Figure 3. DSC thermograms (2nd heating scan) of (a) PLA, and PLA/*m*-silica bio-composite films at various *m*-silica compositions: (b) 1.0, (c) 1.5, (d) 2.0, (e) 2.5, and (f) 5.0 wt%.

Results from the 2nd heating scan also show a similar trend to that from the 1st heating scan. All samples have a semi-crystalline structure with T_g from 59-61 °C, and T_m from 150-152 °C. T_c is observed at approximately 119-121 °C for films containing *m*-silica with a composition from 0 to 2.0 wt%. This slightly increases to 123 and 124 °C for those containing 2.5 and 5.0 wt% *m*-silica compositions, respectively.

Results on the thermal properties of PLA, PLA/*c*-silica, and PLA/*m*-silica bio-composite films, derived from DSC thermograms, are summarized in Table 2. From 1.0 to 5.0 wt% of *m*-silica contents, no significant difference in crystallinity (X_c) of bio-composite films (19-21%) is observed when the silica contents are varied. However, the films with *m*-silica particles exhibit lower T_c, compared to the corresponding films containing unmodified silica. At both 2.5 and 5.0 wt% of particle compositions, PLA/*c*-silica bio-composite films show lower X_c values than neat PLA. This is due to the larger particle size and the presence of aggregates in the unmodified silica, as seen from SEM images. Aggregates are observed in *c*-silica and have a tendency to agglomerate within the PLA matrix. Fillers with smaller particle size provide a larger specific surface, and hence, higher efficiency as nucleating agents for polymer chains. In contrast, the presence of fillers with a large particle size can retard the crystalline formation of polymer chains. c-silica tends to agglomerate and has a larger particle size in composite systems, leading to an increase in T_c and a decrease in X_c of the composite films.

Table 2. Thermal properties of PLA, PLA/*c*-silica and PLA/*m*-silica bio-composite films, derived from DSC thermograms.

Sample	Silica	1st Scan						2nd Scan					
	(%)	T_g (°C)	T_c (°C)	$\Delta(H_c)$ (J/g)	T_m (°C)	$\Delta(H_m)$ (J/g)	*Xc* (%)	T_g (°C)	T_c (°C)	$\Delta(H_c)$ (J/g)	T_m (°C)	$\Delta(H_m)$ (J/g)	*Xc* (%)
PLA	0	60	121	-19	150	19	21	59	124	-18	150	18	19
m-silica	1.0	60	120	-20	149	20	22	59	123	-19	150	19	21
	1.5	61	119	-21	150	21	22	60	122	-20	150	20	22
	2.0	62	121	-20	150	20	21	61	123	-20	150	19	21
	2.5	62	123	-21	150	21	23	59	125	-20	151	20	22
	5.0	62	124	-19	151	20	21	60	125	-19	152	19	21
c-silica	2.5	62	126	-13	151	15	16	60	127	-13	152	14	15
	5.0	61	125	-15	151	15	16	60	125	-19	151	20	21

Tensile behavior of bio-composite films is examined by a Universal Testing Machine (UTM), as summarized in Figure 4. Tensile strength, elongation at break, modulus, and break energy of bio-composites containing *m*-silica and *c*-silica are slightly lower than that of neat PLA film. In fillers/polymer mixtures, filler particles function as a stress concentrator for the matrix. However, this may adversely promote crack initiation if the interfacial adhesion between fillers and the polymer matrix are poor, due mainly to the incompatibility between the 2 components. It is clearly observed that composite films consisting of *m*-silica show greater tensile properties than the corresponding films with *c*-silica. This is due to smaller size and more uniform dispersion of *m*-silica particles in the PLA matrix. The presence of a PCT copolymer coating layer on the silica surface plays a key role in promoting compatibility between *m*-silica and the PLA matrix, and also enhancing dispersion in the composite system.

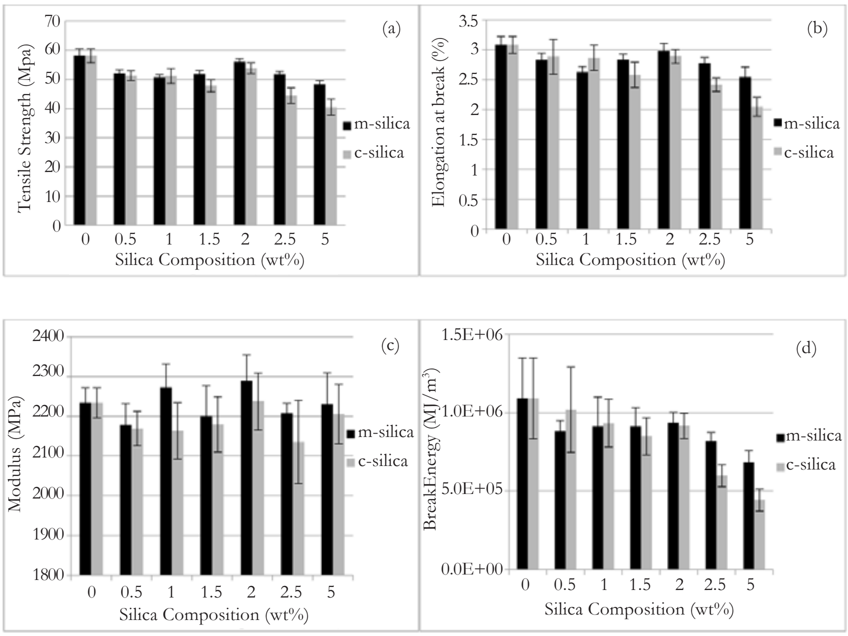

Figure 4. Tensile strength (a), elongation at break (b), modulus (c), and break energy (d) of PLA, PLA/*c*-silica, and PLA/*m*-silica bio-composite films at various silica compositions.

Gas permeability is a crucial factor for packaging design because gases such as oxygen, carbon dioxide, and water vapor have strong effects on shelf-life and quality of foods and fresh products [18]. The requirements for gas permeability of polymer films for a specific product may vary, depending on their activities during storage, such as respiration and oxidation reactions of fresh fruits and vegetables. Those activities produce specific gases such as carbon dioxide (CO_2), oxygen (O_2), and water vapor (WV), which change the atmosphere within the packaging. It is important to study the gas permeability of polymer films in order to ensure effective preservation of products. Gas permeability of the resulting composites films are examined, in terms of oxygen, carbon dioxide, and water vapor permeability, as summarized in Table 3. Water vapor permeability of the composite containing *c*-silica remains significantly unchanged, and that of *m*-silica increases around 2.5 times, compared to neat PLA. This is mainly due to the incorporation of more polar PCT copolymer chains into the hydrophobic PLA matrix. Given that gas diffusion through polymeric films is strongly dependent on size, shape, polarity, and solubility of the gas molecules, the presence of more polar groups in a composite is favorable for polar water molecules [19]. The selectivity value, which represents the permeability ratio of different gases, is also calculated in terms of CO_2/O_2, CO_2/WV, and O_2/WV. Variations in the CO_2/O_2 permeability ratios of bio-composite films are observed with changes in types of silica particles (*c*-silica and *m*-silica) and their compositions. The ratio for PLA/*m*-silica bio-composite films containing 2.5 and

5.0 wt% of *m*-silica are 0.05 and 0.87, respectively, while those of PLA/*c*-silica films are much higher at 9.33 and 2.33, for 2.5 and 5.0 wt% of *c*-silica compositions, respectively.

Table 3. Gas permeabilities: CO_2, O_2, and water vapor (WV), of PLA, PLA/*c*-silica, and PLA/*m*-silica bio-composite films containing different particle compositions.

Sample	O_2 ($cm^3 \cdot mm/m^2 \cdot day \cdot atm$)	CO_2 ($cm^3 \cdot mm/m^2 \cdot day \cdot atm$)	WV ($g/m^2 \cdot day$)	CO_2/O_2	CO_2/ WV	O_2/ WV
PLA	31	25	18	0.81	1.38	1.72
2.5 *m*-silica	183	9	56	0.05	0.16	3.27
5.0 *m*-silica	32	28	53	0.87	0.52	0.61
2.5 *c*-silica	3	28	18	9.33	1.55	0.17
5.0 *c*-silica	15	34	22	2.26	1.54	0.68

It is important to investigate the light transmission behavior of composite films, especially in UV, visible, and near infrared regions, in order to design packaging materials for each food products. Plastic materials tend to undergo photo-chemical degradation when exposed to UV radiation (200-400 nm). Also, food products which exhibit high sensitivity towards visible light tend to spoil in lighting conditions ranging from 400 to 700 nm. Light transmission curves of the composite films, measured by UV-Vis-NIR spectrometry, are shown in Figure 5. Detailed results on %T for PLA/*m*-silica composite films in UV and visible regions are provided in Table 4. The transparency percentage of light (%T) decreases for PLA/*m*-silica composite films, compared to neat PLA, with respect to an increase in the *m*-silica composition. This indicates that *m*-silica particles act as a light absorbing agent for UV (300-400 nm) and Visible (400-765 nm) regions, and prevent the transmission of light through the films. Neat PLA film allows the passage of 72, 83, and 88% of radiation in the UV-A, UV-B, and visible regions, respectively. The %T values tend to decrease in UV regions with increasing *m*-silica content in the bio-composite films. At 5.0 wt% of *m*-silica composition, the film shows a maximum decrease in %T of 4, 8, and 16%, of radiation in UV-A, UV-B, and Visible regions, respectively. The reduction in %T values is due to light absorptivity of chitosan in the PCT copolymer structure, coated on the *m*-silica's surface, which agrees with that reported by Rapa et al [20].

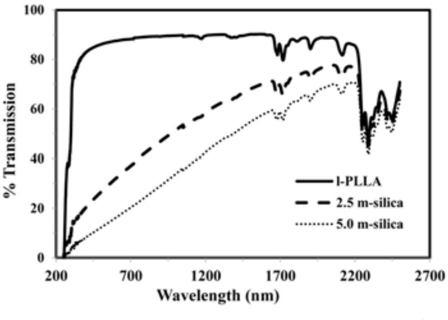

Figure 5. UV-Visible-NIR transmittance spectra of PLA, PLA/*m*-silica bio-composite films at 2.5, and 5.0 wt% compositions.

Table 4. Percentage of light transmission (%T) values for PLA/*m*-silica composite films.

Sample	%Transmittance (%T)		
	at 350 nm (UV-B region)	at 400 nm (UV-A region)	at 600 nm (Visible region)
neat PLA	72	83	88
2.5 *m*-silica/PLA	14	20	32
5.0 *m*-silica/PLA	4	8	16

4. CONCLUSIONS

The surfaces of commercial silica particles (*c*-silica) are successfully modified by coating with PCT copolymer, employing a phase inversion emulsification (PIE) technique. This effective coating step leads to a decrease in average size of the resulting modified silica particles (*m*-silica) to around 17 nm, as a result of steric repulsion from PCT copolymer coated layers, which prevents agglomeration of the silica particles. The resulting modified particles are then successfully used in the preparation of PLA/silica bio-composite films by varying the silica contents (from 0-5.0wt%), and types of silica particles. PLA/*m*-silica films exhibit greater tensile behaviors at all compositions, compared to the correspondingbio-composite films with unmodified *c*-silica particles. The CO_2/O_2 permeability ratio of bio-composite films can be tuned by varying the types of silica particles (*c*-silica and *m*-silica) and their compositions. Light transmission reduction in both the UV and visible regions is achieved in PLA/*m*-silica bio-composite films. The composite films have high potential for use as smart and active packaging.

ACKNOWLEDGEMENTS

The authors acknowledge financial support from the National Research University (NRU) grant, provided from The Office of Higher Education Commission (OHEC) and the Center of Excellence in Materials and Plasma Technology (CoE M@P Tech), Thammasat University. N.J. is grateful for scholarship support from The Royal Golden Jubilee (RGJ) Ph.D. program of the Thailand Research Fund (PHD/0026/2558). The authors gratefully acknowledge the instrument support from Center of Scientific Equipment for Advanced Research, Office of Advanced Science and Technology, Thammasat University.

REFERENCES

[1] Raquez J.M., Habibi Y., Murariu M. and Dubois P., *Prog. Polym. Sci.*, 2013; **38(10)**: 1504-1542. DOI 10.1016/j.progpolymsci.2013.05.014.

[2] Rhim J.W., Hong S.I. and Ha C.S., *Lebenson. Wiss. Technol.*, 2009; **42(2)**: 612-617. DOI 10.1016/j.lwt.2008.02.015.

[3] Imanaka M., Takeuchi Y., Nakamura Y., Nishimura A. and Iida T., *Int. J. Adhes.*, 2001; **21(5)**: 389-396. DOI 10.1016/S0143-7496(01)00016-1.

[4] Urbanczyk L., Ngoundjo F., Alexandre M., Jerome C., Detrembleur C. and Calberg C., *Eur. Polym. J.*, 2009; **45(3)**: 643-648. DOI 10.1016/j.eurpolymj.2008.11.033.

[5] Ouchi T., Ichimura S. and Ohya Y., *Polymer*, 2006; **47(1)**: 429-34. DOI 10.1016/j.polymer.2005.11.039.

[6] Najafi N., Heuzey M.C., Carreau P.J. and Wood Adams P.M., *Polym. Degrad. Stabil.*, 2012; **97(4)**: 554-65. DOI 10.1016/j.polymdegradstab.2012.01.016.

[7] Paul M.A., Alexandre M., Degee P., Henrist C., Rulmont A. and Dubois P., *Polymer*, 2003; **44(2)**: 443-50. DOI 10.1016/S0032-3861(02)00778-4.

[8] Sinha Ray S., Yamada K., Okamoto M., Fujimoto Y., Ogami A. and Ueda K., *Polymer*, 2003; **44(21)**: 6633-46. DOI 10.1016/j.polymer.2003.08.021.

[9] Balakrishnan H., Hassan A., Imran M. and Wahit M.U., *Polym. Plast. Technol. Eng.*, 2012; **51(2)**: 175-92. DOI 10.1080/03602559.2011.618329.

[10] Datta R. and Henry M., *J. Chem. Technol. Biotechnol.*, 2006; **81(7)**: 1119-29. DOI 10.1002/jctb.1486.

[11] Yu L., Dean K. and Li L., *Prog. Polym. Sci.*, 2006; **31(6)**: 576-602. DOI 10.1016/j.progpolymsci.2006.03.002.

[12] Li B., Dong F.X., Wang X.L., Yang J., Wang D.Y. and Wang Y.Z., *Eur. Polym. J.*, 2009; **45(11)**: 2996-3003. DOI 10.1016/j.eurpolymj.2009.08.015.

[13] Yan S., Yin J., Yang Y., Dai Z., Ma J. and Chen X., *Polymer*, 2007; **48(6)**: 1688-1694. DOI 10.1016/j.polymer.2007.01.037.

[14] Ribeiro T., Baleizao C. and Farinha J., *Materials*, 2014; **7(5)**: 3881-3990. DOI 10.3390/ma7053881.

[15] Opaprakasit P., Boonpa S., Jaikaew N., Petchsuk A. and Tangboriboonrat P., *Macromol. Symp.*, 2015; **354(1)**: 48-54. DOI 10.1002/masy.201400117.

[16] Namwong S., Islam M.Z., Noppalit S., Tangboriboonrat P., Chaiyasat P. and Chaiyasat A., *J. Macromol. Sci. Part A*, 2016; **53(1)**: 11-7. DOI 10.1002/masy.201400117.

[17] Zhai W., Ko Y., Zhu W., Wong A. and Park C.B., *Int. J. Mol. Sci.*, 2009; **10(12)**: 5381-5397. DOI 10.3390/ijms10125381.

[18] Mangaraj S., Goswami T.K. and Panda D.K., *J. Food Sci. Technol.*, 2015; **52(9)**: 5456-69. DOI 10.1007/s13197-014-1682-2.

[19] Valentina S., *Int. J. Polym. Sci.*, 2012; **11**. DOI 10.1155/2012/302029.

[20] Rapa M., Mitelup A.C., Tanase E.E., Grosu E., Popescu P. and Popa M.E., *Compos. Part B*, 2016; **102**: 112-121. DOI 10.1016/j.compositesb.2016.07.016.